Paper to be presented at the International Topical Meeting on Sodium Cooled Fast Reactors Safety, Obninsk, Russian Federation, October 3-7, 1994*

SAS4A ANALYSIS OF ABRUPT LOSS OF FLOW WITHOUT SCRAM IN METALLIC FUELED FAST REACTORS

E. E. Morris, A. M. Tentner, and J. E. Cahalan

Reactor Analysis Division
Argonne National Laboratory
9700 S. Cass Avenue
Argonne, IL 60439

*Work supported by the U. S. Department of Energy, Nuclear Energy, Nuclear Energy Programs under Contract W-31-109-ENG-38.

SAS4A ANALYSIS OF ABRUPT LOSS OF FLOW WITHOUT SCRAM IN METALLIC FUELED FAST REACTORS

E. E. Morris, A. M. Tentner, and J. E. Cahalan
Reactor Analysis Division
Argonne National Laboratory
9700 S. Cass Avenue
Argonne, IL 60439 USA
(708) 252-4687

ABSTRACT

The energetics potential of severe accidents is investigated for a large sodium cooled, metallic-fueled fast reactor using the SAS4A accident analysis code. The accident initiator considered is an abrupt loss of flow with failure to scram. Extensive analysis of the response of metallic fueled reactors to double fault initiators such as loss of flow, loss of heat sink, or transient overpower with failure to scram shows that the reactors passively adjust their power to match the available heat rejection capability without boiling coolant or melting fuel. The analysis considered here assumes some extremely unlikely additional contribution to the accident such as the failure of the flow-coastdown mechanism. The reactivity insertion rate due to coolant voiding and the low melting point of metallic fuel cause fuel to disperse within intact cladding prior to cladding failure. Negative reactivity feedback from this in-pin fuel motion counters the positive reactivity insertion and prevents a rapid and large release of energy. The SAS4A analysis shows that extensive core melting and disruption can be expected, but that the energy release will not be large enough to threaten rupture of the reactor vessel. Metallic fuel acts as an additional safety device which acts to counter large or rapid reactivity insertions.

I. INTRODUCTION

The SAS4A accident analysis code[1] has been used to investigate the energetics potential of severe accidents initiated by abrupt loss of flow without scram in metallic fueled reactors. Extensive analysis of the response of metallic fueled reactors to double fault initiators such as loss of flow, loss of heat sink, or transient overpower with failure to scram have shown that the reactors passively adjust their power to match the available heat rejection capability without boiling coolant or melting fuel.[2,3] Results for the loss-of-flow and loss-of-heat-sink sequences have been confirmed in full-scale tests in the EBR-II reactor.[4] A search for accident initiators potentially leading to energetic core disruption identified the abrupt loss-of-flow sequence as the most likely candidate. Analysis of this sequence assumes that the primary coolant pumps stop instantaneously, leading to a very rapid reduction in flow, and that the reactor scram system fails to operate. This initiator is extremely unlikely, but could perhaps be caused by a very large earthquake which causes the coolant pump rotors to seize or breaks coolant pipes feeding the inlet plenum. The SAS4A analysis shows that extensive core melting and disruption could be expected. However, the amount of energy released during the reactivity excursion would not be sufficient to threaten the reactor vessel, and thus would not pose a safety risk to persons in the vicinity of the reactor.

II. REACTOR MODELING

The abrupt-loss-of-flow analysis was performed for the metallic fueled 3500-MWt, pool-type reactor analyzed previously in a recent joint study with the European liquid metal-cooled research and development community.[2,3] Table I shows some of the more important characteristics of the reactor. Figure 1 shows a plan view of the core layout.

The SAS4A model was expanded from the three-channel model constructed for the analysis described in Refs. 2 and 3 to a 25-channel model. Each channel represents a single surrogate fuel pin along with associated coolant and structure from a group of assemblies which for purpose of analysis are assumed to be identical. SAS4A performs a detailed thermal-hydraulic analysis and fuel motion calculation for each surrogate fuel pin. All fuel pins within an assembly group are assumed to behave like the surrogate pin for that group.

TABLE I. Reactor Description

Core Power, MWt	3500
Core Height, in	36
Assembly Pitch, in	6.131
Assembly Outer Flat-to-Flat, in	5.931
Assembly Wall Thickness, in	0.150
Driver Fuel Composition	U-15Pu-10Zr
Number of Driver Assemblies	396
Number of Blanket Assemblies	163
Driver Pins per Assembly	271
Blanket Pins per Assembly	169
Wire Wrap Pitch, in	12
Driver Pin Outside Diameter, in	0.285
Driver Cladding Thickness, in	0.022
Driver Wire Wrap Diameter, in	0.049
Driver Smear Density, % T.D.	75
Blanket Pin Outside Diameter, in	0.392
Blanket Cladding Thickness, in	0.022
Blanket Wire Wrap Diameter, in	0.034
Blanket Smear Density, % T.D.	85
Fission Gas Plenum Length, in	52
Coolant Outlet Temperature, °C	510
Coolant Temperature Rise, °C	153
Primary Control Rods	24
Secondary Control Rods	12
Driver Linear Power, kW/ft*	12.6
Driver Sodium Void Reactivity, $*	4.98
Blanket Sodium Void Reactivity, $*	2.31
Driver Doppler Coefficient**	1.93
Blanket Doppler Coefficient**	1.73
Delayed Neutron Fraction*	0.00352
Prompt Neutron Lifetime, 10^{-7} s*	3.20

* End of Equilibrium Cycle
** $-10^{-3}\ T\ dk/dT$, End of Equilibrium Cycle with Sodium In

Neutronics calculations produced axial power shapes and reactivity worth distributions for each of 63 distinct fuel, internal blanket, and radial blanket assemblies in a one-twelfth sector of the core. The 25-channel model represents the 55 fuel and internal blanket assemblies. The power and worth distributions were averaged over all assemblies in an assembly group and the averages assigned to the channel representing the group. Figure 2 shows that the assembly power distribution for the 25-channel model provides a very good representation of the original 55-assembly fuel and internal blanket power distribution.

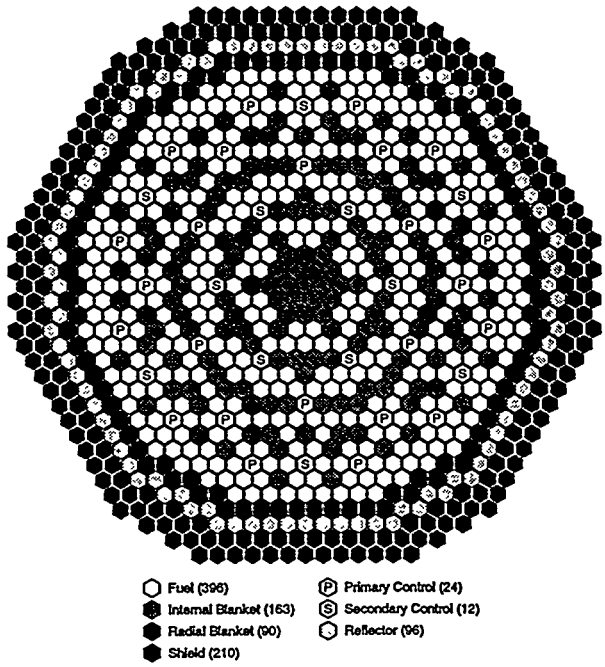

Fig. 1. Plan view of the reactor core.

III. SAS4A RESULTS

Prior to fuel melting, all the transients considered below have a common event sequence. The calculations simulate the abrupt loss of flow by assuming that all primary pumps seize at time zero. Following seizure, coolant flow through the core decays with a 160 ms halving time. Coolant boiling and voiding begins within 2.2 s. Coolant voiding introduces positive reactivity at rates which approach 10 to 12 $/s at the time when fuel melting and motion begin. The reactivity approaches

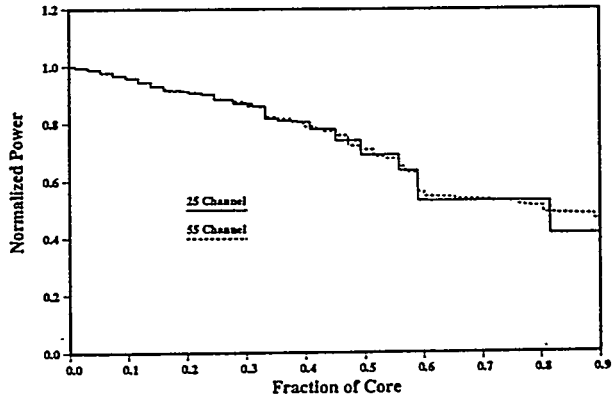

Fig. 2. Fraction of core with power greater than the normalized power.

prompt critical, but Doppler and fuel pin axial expansion feedback arrest the reactivity rise short of prompt critical.

Events following the onset of fuel melting depend on conditions near the top of the fuel pin. Because of the low melting point of the metallic fuel, a significant inventory of molten fuel develops before cladding fails. This fuel resides in a molten cavity within the fuel pin. Because of the abruptness of the loss of flow, the formation of the cavity is biased toward the core midplane. In spite of the bias, the fuel temperature near the top of the fuel pin reaches solidus before cladding failure and is expected to allow the cavity fission gas pressure to push fuel upward through the intact cladding into the fission gas plenum. This rapid in-pin fuel motion drives the reactivity downward. Subsequent cladding failures tend to occur close to the core midplane, and initially positive reactivity feedback results as the fuel moves within the fuel pin toward the failure site and through the cladding breach into the coolant channel. Because of the reactivity reduction caused by the in-pin motion prior to cladding failure, the positive feedback caused by the failure does not drive the reactor prompt critical, and dispersal of the fuel through the coolant channels soon renders the reactor subcritical.

A. Reference Case

In the reference calculation, the fission gas and fill gas were set to provide a pin pressure of 1.44 MPa at a reference temperature of 300 K. Since the fill gas alone provides a pressure of 0.1 MPa, this pressure corresponds to a core-wide average burnup of about 6.5 atom %. Through input, the PINACLE module in SAS4A initiated fuel motion when the fuel reached 40% of it heat of fusion over an areal fraction of 20% in the peak axial node and 10% in the two adjacent nodes. Fission gas was allowed to migrate so as to maintain a uniform axial pin pressure during steady state, but migration was not permitted once the transient started. Rapid in-pin motion began when the molten fuel cavity reached the top axial computational node of the fuel pin, and after the temperature in the node reached solidus.

Figure 3 shows the the power and reactivities during the first 2.4 s. Following seizure of the pump rotors, flow falls rapidly, but the gravitational head of cold coolant between the heat exchanger and the inlet plenum prevents the coolant flow from dropping all the way to zero. The resulting coolant heat-up produces positive reactivity feedback and leads to a gradual increase in the reactor power. The initiation of coolant boiling just before 2.2 s causes flow reversal at the inlet of several fuel assemblies, and the rapid introduction of the voiding

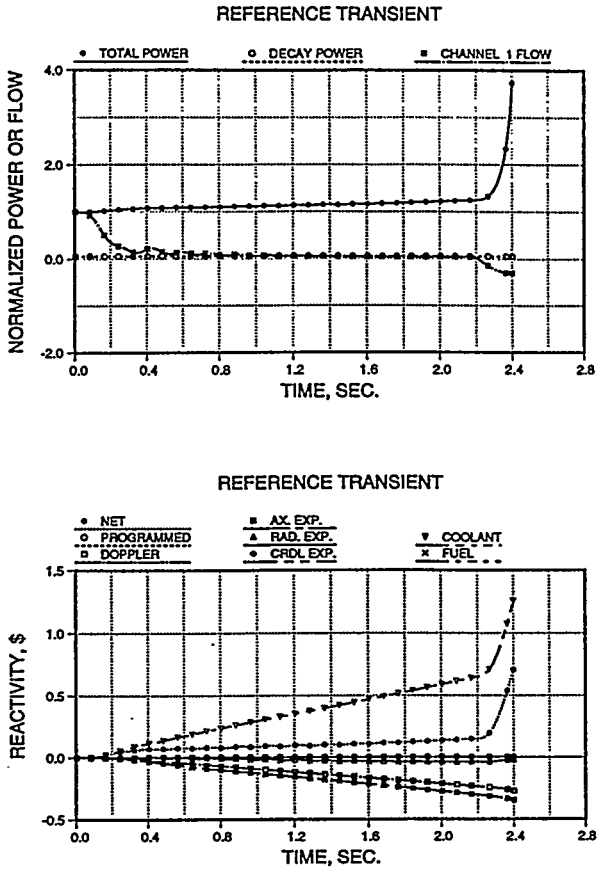

Fig. 3. Power and reactivities.

reactivity feedback causes the power to rise sharply. The initial growth of the voided region is shown for the highest powered fuel assemblies in Fig. 4. The top and bottom of the core are located at about 1.02 and 0.1 m respectively. The figure shows that voiding begins between 0.1 and 0.15 m above the axial midplane, and that the voiding is preferentially toward the top of the

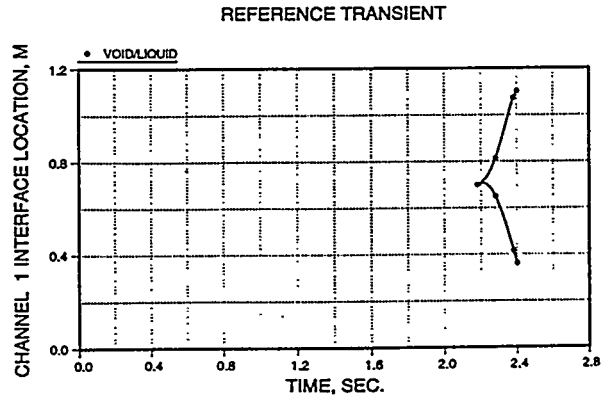

Fig. 4. Initial top and bottom void interfaces.

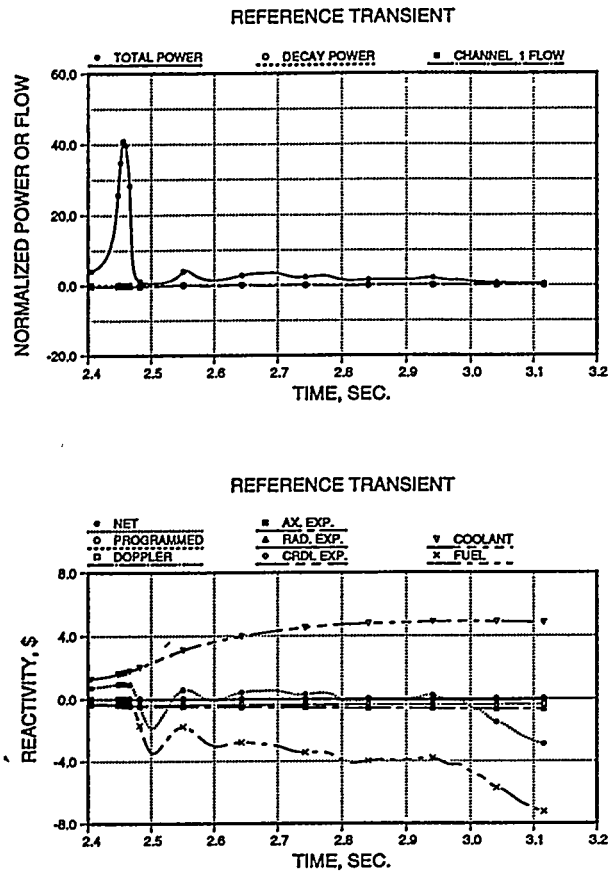

Fig. 5. Power and reactivities.

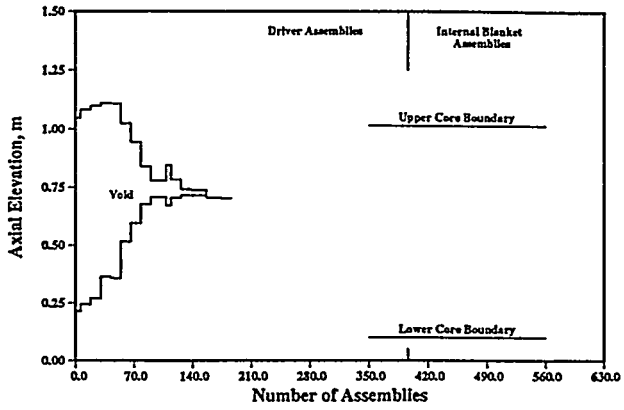

Fig. 6. Void pattern at 2.46 s.

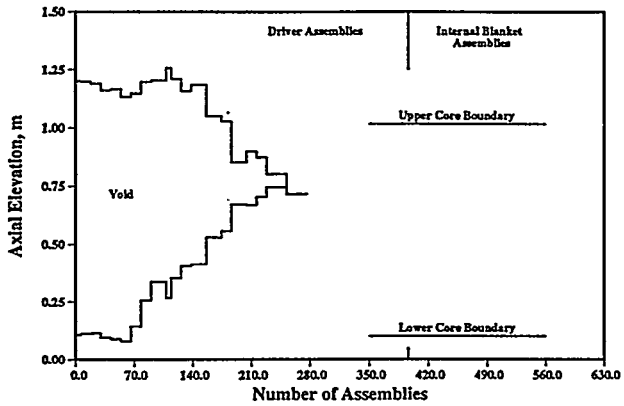

Fig. 7. Void pattern at 2.55 s.

core. Voiding initiates in channels 1 through 13, representing 39% of the core, between 2.18 and 2.43 s.

Figure 5 shows the power and reactivities for the remainder of the reference transient. Molten cavities in channels 1 through 22, representing 83% of the fuel assemblies, between 2.435 and 2.47 s. Rapid in-pin motion initiates in 8 channels, representing 23% of the core, in a 7 ms time period starting at 2.462 s. The net reactivity is 0.95 $ and the power level has reached 36 times nominal when the rapid in-pin motion begins. The rapid in-pin motion contributes more than 3 $ of negative fuel motion reactivity within about 40 ms. Following this initial negative reactivity insertion, some of the fuel reenters the core and, in combination with the continuing increase in the coolant voiding reactivity, drives the net reactivity to about 0.6 $. At about 2.57 s, more fuel is ejected from the core, helped by the initiation of rapid in-pin motion in channels 7, 8, and 11, representing 36 additional fuel assemblies. Cladding failures occur in channels 1 through 7 and in channels 9, 14, and 15 between 2.89 and 3.10 s. These channels represent 32% of the fuel assemblies. Each failure occurs within about 0.16 m of the core midplane and contributes positive fuel motion reactivity feedback for about 30 ms following failure. There is enough temporal separation of the failures to prevent the positive feedbacks from driving the reactor near prompt critical. The calculation stopped with the reactor subcritical and the power level approaching 0.4 times nominal. Additional fuel melting and cladding failures can be expected, but they are not likely to add greatly to the energy deposited. Peak fuel temperatures at the end of the calculation are well below 2000 K.

The "snap shots" in Figs. 6 through 9 show the extent of core voiding at four different times during the reference transient. The area of the region labeled "void" is proportional to the core void volume. The assemblies are grouped in order of ascending channel number. Thus, the first six assemblies represent channel 1, the next 12, channel 2, and so on. The snap shot at 2.46 seconds indicates the voiding pattern at the time when rapid in-pin motion begins, and that at 2.88 s shows that pattern just before the first cladding failure. The times 2.55 and 2.68 s are arbitrarily selected intermediate times. The figures show that voiding does not initiate in the internal blanket assemblies. The physical picture of the reactor core at the

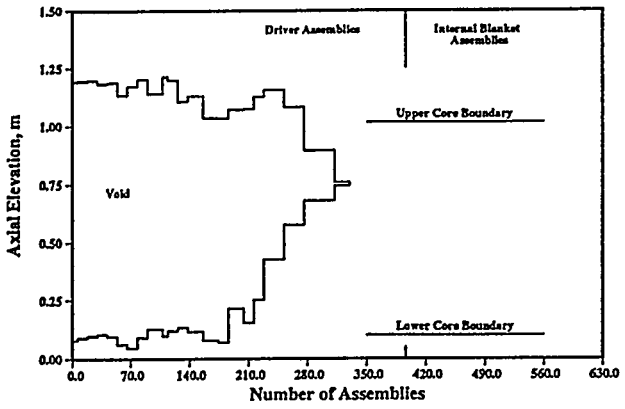

Fig. 8. Void pattern at 2.68 s.

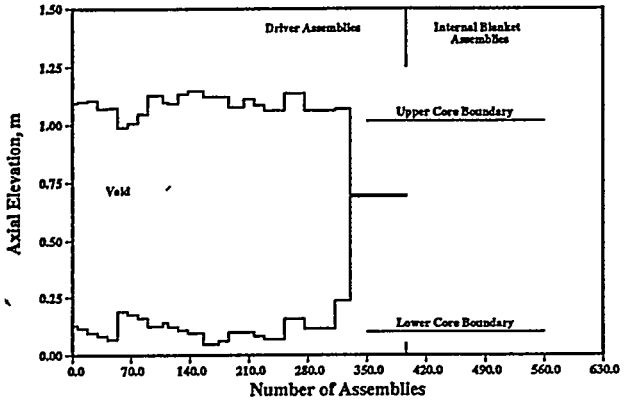

Fig. 9. Void pattern at 2.88 s.

time of cladding failure is of fully flooded blanket assemblies sitting in regions with fully or substantially voided fuel assemblies.

Among the factors which influence the time of cladding failure are the cladding temperature and heating rate, the pressure difference between the inside of the fuel pin and the coolant channel, and the thinning of the cladding due to eutectic formation at the fuel/cladding interface. Figure 10 shows the cladding temperature as a function of axial position just prior to the power peak in Fig. 5 (2.41 s), just prior to cladding failure in a high-powered fuel assembly (channel 1 at 2.89 s) and at an intermediate time (2.70 s). The curves show that the cladding temperature has its maximum value near the axial elevation where the cladding fails. The curves also indicate an average heating rate of about 500 K/s over the time period just prior to cladding failure. The code predicts cladding failure on the basis of a life fraction correlation of data including heating rates up to a few hundred K/s.[5]

The plot in Fig. 11 shows the pressure difference between the inside of the fuel pin and the

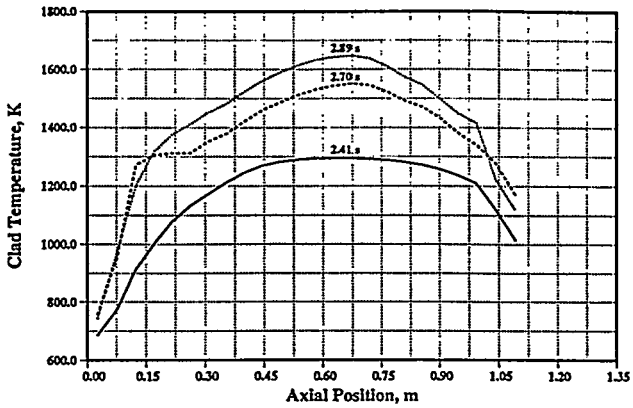

Fig. 10. Selected cladding temperatures in the highest powered subassembly.

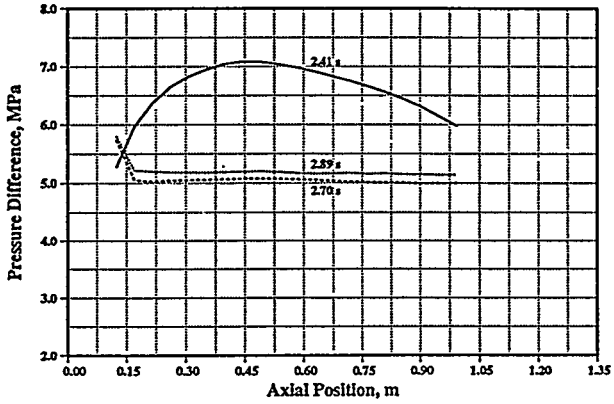

Fig. 11. Selected pressure differences in the highest powered subassembly.

adjacent coolant channel for a high-powered fuel assembly (channel 1) at the same three times considered in the cladding temperature plots. The pressure shows a significant variation with axial position prior to the initiation of rapid in-pin fuel motion. Following the start of rapid in-pin fuel relocation, the pressure difference decreases and becomes axially uniform. The higher pressure at the bottom of the fuel pin reflects the fact that fuel in this part of the pin is not yet mobile.

Figure 12 shows the effect of eutectic formation on the cladding thickness. The times for the plotted results are the same as considered for the cladding temperature plots in Fig. 10. The cladding thickness has it minimum at about the same axial location where the temperature has its maximum, the position where the life fraction criterion predicts cladding failure. The application the life fraction correlation to a situation where a pressurized cladding tube is both heating and changing wall thickness because of eutectic formation has not been verified, and is a source of uncertainty in the reference calculation.

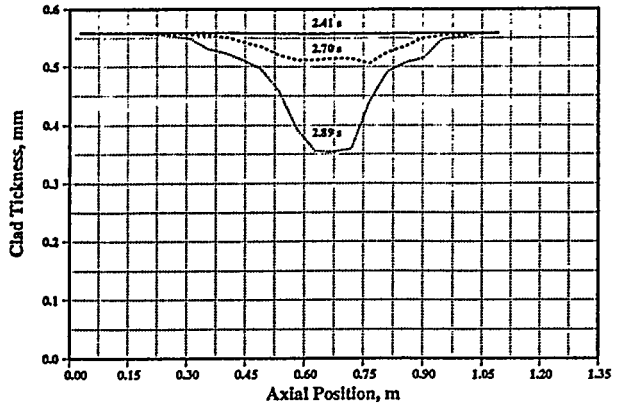

Fig. 12. Selected cladding thicknesses in the highest powered subassembly.

B. Parametric Cases

Several parametric cases assess sensitivity of the calculated results to the input assumptions used in the reference case. Cases 1 and 2 explore sensitivity to the burnup. In Case 1, the sum of the partial pressures of fill and fission gases was set to 0.306 MPa, corresponding to a burnup of about one atom %, and in Case 2, the sum was set to 3.19 MPa, corresponding to a burnup of about 15 atom %. One atom % is about the burnup at which the steady state axial expansion of the fuel stops and gas release begins.[6] At this burnup, the fuel has expanded radially out to the cladding. Fifteen atom % burnup is representative of a high-burnup situation. Axial variation of the burnup is not taken into account and as in the reference case all fuel assemblies are assumed to have the same burnup.

The plots in Fig. 13 compare the powers and net reactivities computed in Cases 1 and 2 with the values from the reference transient. The results show that the effect of changing the burnup is to change the time scale of the accident following the initiation of rapid in-pin fuel motion. All three cases initiate rapid in-pin fuel motion within 2 ms of one another; however, the pressure difference between the fuel pin cavity and the fission gas plenum is smaller in the low-burnup case, and a more gradual introduction of fuel relocation reactivity feedback results. This leads to greater energy deposition during the first power excursion. It also results in the initiation of rapid in-pin fuel motion in about 40% of the fuel assemblies before the local minimum in the reactivity at about 2.55 *s*. In both the reference transient and in Case 2, rapid in-pin fuel motion begins in only about half as many fuel assemblies before the local minimum in the fuel motion reactivity feedback. The larger energy release in the first power excursion and the initiation of rapid in-pin fuel motion in more fuel assemblies cause Case 1 to have

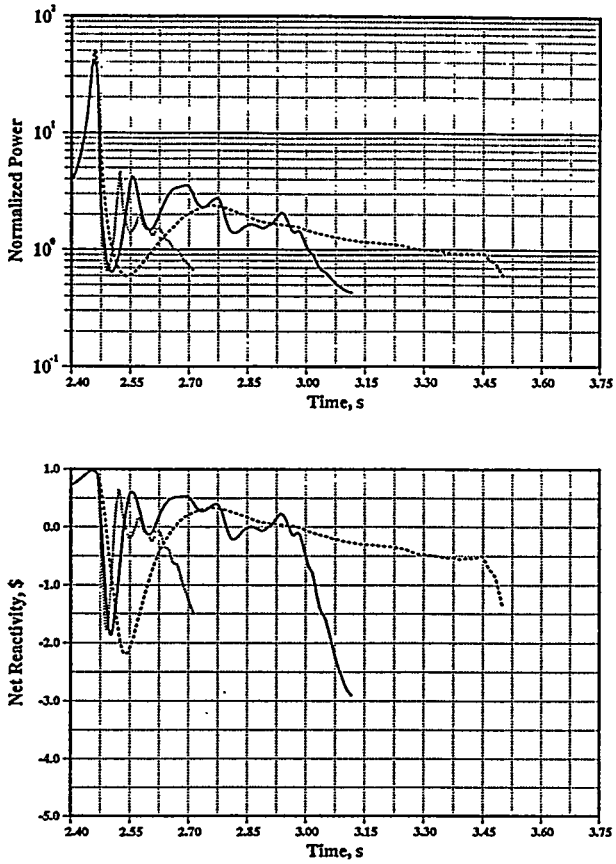

Fig. 13. Comparison of powers and reactivities for Case 1 (dashed curve) and Case 2 (dotted curve) with the Reference Case (solid curve).

a deeper minimum in the fuel motion reactivity feedback than in the higher burnup cases.

Cladding failures must occur to provide sufficient negative reactivity feedback to completely offset the positive void reactivity. The lower fission gas pressure in the low-burnup case causes a longer time interval between the initiation of rapid in-pin fuel motion and the first cladding failure. The corresponding time intervals are 933 ms in the low-burnup case and 34 ms for the high-burnup case. The interval in the reference transient is 430 ms. The longer time interval along with similar power levels following the initial power excursion cause the larger energy release in the low-burnup case. Both Cases 1 and 2 end with peak fuel temperatures less than 2000 K and the energy release poses no threat to the reactor vessel.

Case 3 differs from the reference transient in that fission gas migration sufficient to maintain an axially uniform gas pressure within the fuel pin continues up until the time when fuel melting begins and a cavity of molten fuel and fission gas forms. This reduces by nearly a

factor of two the amount of gas in the central parts of the fuel pin at the time when rapid in-pin fuel motion initiates and has the related consequence that a significantly smaller amount of fuel must be ejected to equilibrate the pressure in the molten cavity with the pressure in the fission gas plenum. The plots in Fig. 14 compare power and net reactivity for Case 3 with the reference case. The reduced amount of fission gas causes a larger amount of energy to be deposited in the initial power excursion and leads to a slightly larger voiding rate following the excursion. More importantly, the lower gas concentration results in less negative fuel motion reactivity feedback from the channels where rapid in-pin fuel motion first occurs, and, during the subsequent fuel reentry, the feedback reaches a local maximum that is about 0.7 or 0.8 $ higher than in the reference transient. The combination of the higher voiding rate and the larger local maximum causes the net reactivity to over shoot prompt critical and causes a second power excursion which terminates when several more channels initiate rapid in-pin fuel motion and produce large negative fuel relocation feedback. Cladding failures begin to occur just after 2.57 s, but the positive fuel motion feedback is not sufficient to overcome the negative feedback caused by the rapid in-pin fuel motion. The reactor remains sub-critical.

Fission gas migration subsequent to pump seizure causes the reactivity to exceed prompt critical briefly in Case 3. The reentry of fuel following ejection to the fission-gas plenum causes prompt-criticality to be reached earlier in the transient, but suppression of reentry does not prevent prompt-criticality. This is confirmed by Case 4 which repeats Case 3 with reentry prohibited. The results from this case are compared with Case 3 and the reference transient in Fig. 14. Following the reactivity decrease caused by the initiation of rapid in-pin fuel motion, the coolant voiding reactivity feedback gradually pushes the net reactivity back into the 0.3 to 0.6 $ range. Rapid in-pin fuel motion initiates in several additional fuel assemblies starting around 2.57 s, but the continued increase of voiding reactivity feedback offsets the resulting negative reactivity feedback, and the net reactivity levels off until cladding failures begin around 2.76 s. The positive fuel relocation feedback following cladding failure drives the net reactivity over prompt critical and causes a second power excursion just before 2.8 .s. The energy release during this power excursion is not as large as during the second excursion in Case 3. Both Cases 3 and 4 have energy releases larger than in the reference transient and produce peak fuel temperatures in the neighborhood of 2500 K. These temperatures are well below the temperature required to produce significant fuel vapor pressure (~ 3500 K) and do not pose an immediate threat to the reactor vessel.

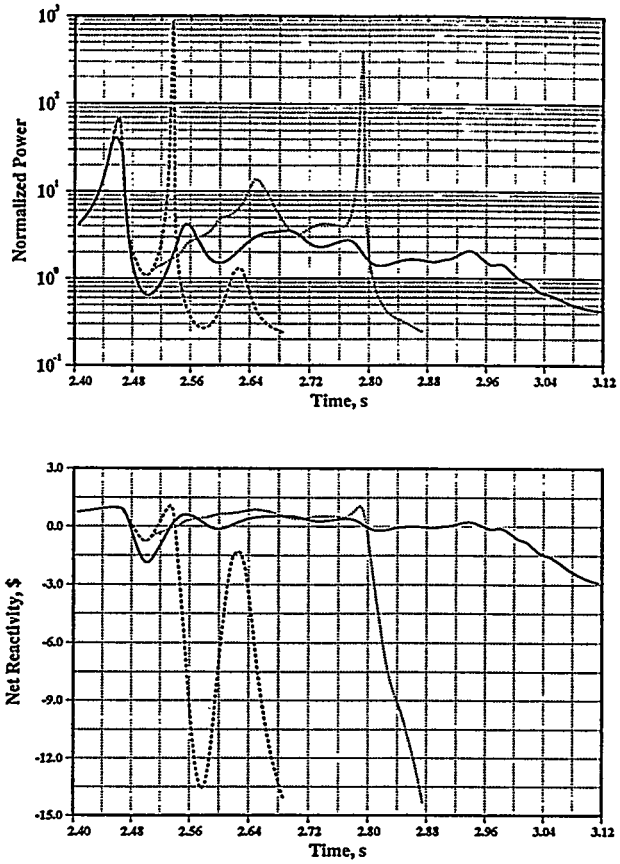

Fig. 14. Comparison of powers and reactivities for Case 3 (dashed curve) and Case 4 (dotted curve) with the Reference Case (solid curve).

Additional parametric cases include exploration of the sensitivity to the criterion used to initiate rapid in-pin fuel motion. The SAS4A heat transfer model does not currently account for heat conduction between the top of the fuel and the bond sodium displaced into the fission gas plenum. The code initiates rapid in-pin fuel motion when the temperature at the interface between the top of the fuel and the bottom of the displaced bond sodium reaches the fuel solidus temperature and the when the molten fuel cavity is calculated to extend into the top axial computational node. A separate calculation of the transient heat conduction near the interface between a semi-infinite medium of fuel and a semi-infinite medium of sodium indicates conductive heat transfer is negligible for the heating rates implied by the power levels in the cases considered so far. Thus, for the cases considered so far, the code estimated the interface temperature as the fuel temperature at the centerline of the top axial computational node. This means that the extension of the molten cavity into the top axial node controls the initiation of rapid in-pin fuel motion. One parametric case repeated the reference transient with the input modified to estimate the interface temperature as the average of the displaced

bond sodium temperature and the centerline temperature of the top axial node of the fuel. The resulting delay in the start of rapid in-pin fuel motion caused fewer fuel assemblies to initiate in-pin fuel motion prior to cladding failure and resulted in an energetic transient. Because of the high heating rates, the estimation of the interface temperature as the temperature at the centerline of the top axial node appears to be more reasonable than using the average temperature as the estimate. Additional considerations suggested by Sevy[7] indicate that even this criterion may delay the onset of rapid in-pin fuel motion unnecessarily. The next section provides additional discussion of this point.

IV. PHENOMENOLOGICAL CONSIDERATIONS

Two primary phenomenological considerations hold the key to a non-energetic outcome for the initiating phase, particularly for the sudden-loss-of-flow accident. The first is the initiation of fuel relocation to the fission gas plenum, and the second the absence of significant fission gas relocation within the fuel pin during the transient. A third consideration, the return of fuel to the core after ejection to the plenum, may be important if either of the first two considerations cannot be resolved favorably. Theoretical calculations by Gesh and Kramer[8] provide firm support for the absence of fission gas relocation. Additional sophistication in the modeling of the interface between the top of the fuel and the fission gas plenum may provide additional insight into the first and third considerations, but experimental support is highly desirable for the ultimate resolution of these issues.

The calculations described in Sect. III initiated fuel relocation to the fission gas plenum when both the centerline temperature of the top axial node in the fuel reached the fuel solidus temperature and the molten cavity extended into the top axial computational node for the fuel. If fuel was assumed to remain immobile until it absorbed 40% of the heat of fusion, then the extension of the cavity to the top computational node was the controlling criterion. At the time when this criterion was satisfied, the fuel temperature had reached solidus across the full radial extent over a significant axial length of the fuel pin. Sevy[7] has postulated that the relatively large pressure difference between the fuel pin cavity and the fission gas plenum, particularly at the higher burnups, would probably initiate fuel displacement to the fission gas plenum even before fuel has melted all the way out to the cladding. An earlier initiation of fuel relocation was simulated in a couple of cases (not described in Sect. III) by reducing the fraction of the heat of fusion required for the fuel to become mobile. One of these cases showed that the earlier initiation had the potential to make the higher burnup cases less sensitive to the timing of cladding failures. Experimental support for the modeling of the initiation of rapid in-pin fuel relocation is highly desirable.

Fission gas migration during the transient was not allowed in most of the cases described in Sect. III. The cases where gas migration was permitted up until the initiation of fuel melting and cavity formation produced significantly higher fuel temperatures than cases where migration was not permitted. This result obtained at all burnups, showing that the issue is not only the total amount of fission gas in the fuel pin, but also the relative amounts of gas in the pin and gas plenum. Smaller amounts in the pin relative to the plenum require smaller displacements of fuel to bring the cavity pressure into equilibrium with the pressure in the plenum. This in turn means less negative feedback to offset the positive feedback that follows cladding failures. Calculations by Gesh and Kramer[8] show that gas is not able to relocate within the fuel pin on the time scale of a few seconds, indicating assumption of no gas migration is reasonable.

The return of fuel to the active core following ejection to the fission gas plenum has the potential to cause oscillations in the fuel motion reactivity feedback, particularly following high overpower conditions. Cladding failures coincident with the return of fuel to the core can augment the already increasing feedback and lead to high overpower conditions. Parametric calculations indicate that the accident consequences are insensitive to the possible reentry of fuel after ejection provided there is sufficient time between the initiation of ejection to the gas plenum and the first cladding failures, and so long as gas migration within the fuel does not occur during the transient. It should further be noted that parametric cases in which the fuel became mobile when the fuel reached 10% or less of its heat of fusion (not discussed in Sect. III) had increased fuel viscosity when rapid in-pin motion began. The higher viscosity essentially eliminated the tendency for the fuel to reenter the core after ejection. If the lower mobility limit is reasonable, as seems likely, and if the viscosity used in the calculation is reasonable, the question of allowing or not allowing fuel reentry may become moot.

V. CONCLUSIONS

An essential part of the scenario for sudden-loss-of-flow accidents is that enough fuel relocates to the fission gas plenum so that when cladding failures occur, the resulting positive feedback will not drive the reactor into an energetic power excursion. In Sect. III, the criterion used for the initiation of rapid in-pin fuel motion seems to

be conservative since, as discussed in Sect. III and Sect. IV, a less restrictive criterion seems justifiable. Thus, the requirement for sufficient fuel relocation to the fission gas plenum prior to cladding failure seems readily met. The sequence of events in the reference transient for the 3500-MWt reactor is representative of what would be expected in all abrupt loss-of-flow transients. Peak fuel temperatures were much less than 2000 K and considerably less than the temperature required to produce significant fuel vapor pressure. In parametric cases, several input assumptions which were thought to have the potential for upsetting the desired event sequence were changed. These cases demonstrated that, while it is easier to disrupt the desired event sequence at the higher burnups, the event sequence found in the reference transient is likely to hold for the entire range of burnups above about 1 atom %.

The calculations described above have been carried out for smaller reactors and for reactors with lower void worths. While the response for these reactors differ somewhat in the accident sequence details, the overall results are very similar. In general, the rapid loss-of-coolant flow leads to spatially coherent coolant boiling and voiding. The power increase brought about by the positive coolant voiding reactivity, and the loss of cooling due to the flow stoppage, result in fuel heating and melting with the cladding intact. When fuel melting opens a flow path between the high-pressure molten fuel cavity and the lower-pressure fission gas plenum above the core, a rapid in-pin relocation of fuel results. The reactivity effect of this fuel motion is strongly negative, and acts to counter the positive reactivity coming from coolant voiding. Subsequent cladding failures occur at reduced power and reactivity levels, and fuel ejection and relocation after cladding failures render the core permanently subcritical. This general behavior comes about because the metallic fuel melting temperature is lower than the cladding melting temperature, so in-pin fuel relocation will precede cladding failure in the sudden loss-of-flow sequence. Metallic fuel thus provides a "fuse" or "circuit breaker" to counter the impact of positive coolant voiding reactivity, and to render the loss-of-flow accident sequence non-energetic, with no potential for breaking the reactor vessel, and a very low risk to the public safety.

ACKNOWLEDGEMENTS

R. H. Sevy worked out the basic event sequence for the sudden-loss-of-flow accident in a set of scoping, hand calculations. We benefited greatly from numerous discussions with him as this work progressed.

This work was supported by the U. S. Department of Energy, Nuclear Energy Programs under contract W-31-109-ENG-38.

REFERENCES

1. J. E. Cahalan, et al, "Advanced LMR Safety Analysis Capabilities in the SASSYS-1 and SAS4A Computer Codes," Proceedings International Topical Meeting on Advanced Reactor Safety, Pittsburgh, Pennsylvania, USA, Volume 2, pp. 1038-1045, April 17-21, 1994.

2. J. E. Cahalan, et al, "Performance of Metal and Oxide Fuels During Accidents in a Large Liquid Metal Cooled Reactor," Proceedings of the International Fast Reactor Safety Meeting, Snowbird, Utah, USA, Volume IV, pp. 73-82, August 12-16, 1990.

3. P. Royl, et al, "Influence of Metal and Oxide Fuel Behavior on the ULOF Accident in 3500 MWth Heterogeneous LMR Cores and Comparison with Other Large Cores," Proceedings of the International Fast Reactor Safety Meeting, Snowbird, Utah, USA, Volume IV, pp. 83-92, August 12-16, 1990.

4. H. P. Planchon, et al., "Implications of the EBR-II Inherent Safety Demonstration Test," Nucl. Eng. Des., 101(1), pp. 75-90, January, 1987.

5. M. L. Hamilton, et al, Private Communication, 1986.

6. E. E. Gruber and J. M. Kramer, Private Communication, 1988.

7. R. H. Sevy, Private Communication, 1993.

8. C. Gesh and J. M. Kramer, Private Communication, 1987.